Journal of Molecular Catalysis A: Chemical 346 (2011) 20–28

Contents lists available at ScienceDirect

Journal of Molecular Catalysis A: Chemical

journal homepage: www.elsevier.com/locate/molcata

Investigation of iron complexes in ATRP: Indications of different iron species in normal and reverse ATRP

Helena Bergenudd[a,*], Mats Jonsson[a], Eva Malmström[b]

[a] Nuclear Chemistry, KTH Chemical Science and Engineering, Royal Institute of Technology, SE-100 44 Stockholm, Sweden
[b] Fibre and Polymer Technology, KTH Chemical Science and Engineering, Royal Institute of Technology, SE-100 44 Stockholm, Sweden

ARTICLE INFO

Article history:
Received 28 March 2011
Received in revised form 30 May 2011
Accepted 2 June 2011
Available online 12 June 2011

Keywords:
Atom transfer radical polymerization (ATRP)
Kinetics
Electrochemistry
Iron catalyst

ABSTRACT

In an attempt to correlate the ATRP kinetics and the redox properties of the mediator, eight iron complexes with nitrogen, phosphorous and carboxylic acid containing ligands were investigated by electrochemical measurements and by using them as mediators in normal and reverse ATRP of MMA in DMF. The redox properties of the iron complexes in DMF, measured by cyclic voltammetry, did not differ significantly, which was reflected in the ATRP kinetics as the apparent rate constants were practically the same with all the complexing ligands. The degree of control over the polymerization was, however, much improved in reverse ATRP as compared to normal ATRP. In this ATRP system, the ligand type is not crucial for the redox or polymerization properties. Several observations indicate that the iron species in the two systems were not the same, the Fe(III) species resulting from oxidation of Fe(II) in normal ATRP is different from the starting Fe(III) species in reverse ATRP.

1. Introduction

Atom transfer radical polymerization (ATRP) is one of the most commonly employed techniques for controlled radical polymerization [1–3]. Control over molecular weight and a low degree of termination requires a low concentration of radicals. In ATRP, this is realized through an equilibrium between the dormant polymer chain (RX) and the corresponding polymer radical ($R^{\bullet}$), mediated by a transition metal complex (activator) (Scheme 1). The equilibrium should be shifted towards the dormant species to keep the radical concentration sufficiently low to minimize termination reactions. The reduction potentials of the alkyl halide (dormant polymer chain) and the transition metal complex, together with the halidophilicity (halogen affinity) of the oxidized transition metal complex, all being part of the equilibrium constant ($K_{ATRP} = k_{act}/k_{deact} = f(E_{RX}, E_{Mt}, K_x)$), are properties of the polymerization system which are crucial for the performance of the polymerization (i.e. the degree of control).

In normal ATRP, the polymerization starts from the initiator (alkyl halide) and the transition metal in its lower oxidation state. Alternatively, it can be started with a conventional radical initiator (e.g. AIBN) and the transition metal in its higher oxidation state, so called reverse ATRP [4]. The radicals arising from the (thermal) dissociation of the initiator are reversibly terminated by the transition metal, hence resulting in an alkyl halide and the reduced transition metal. A third technique is AGET (activators generated by electron transfer) ATRP, where the transition metal is added in its higher oxidation state and is reduced by e.g. ascorbic acid before it can activate the alkyl halide initiator [5].

The environmental aspects of ATRP have gained increased interest in recent years. Many of the employed transition metals (e.g. copper) and ligands are harmful and it is also desirable to reduce the use of hydrocarbon solvents. ARGET (activators regenerated by electron transfer) ATRP has emerged as one way to reduce the amount of copper [6]. Also, ionic liquids have been used in an effort to facilitate the removal of the mediator and as a means to reduce the amount of solvent (through reuse) [7]. The most commonly used transition metal so far is copper, but to use iron complexes as mediators in ATRP is an attractive route to less harmful ATRP systems. A recent review by Ouchi et al. [8] gave an overview of a large number of ATRP mediators, including both iron and copper complexes. Iron has been used in ATRP together with various ligands, e.g. triphenyl phosphine [9–14], diimines and diamines [15,16], imino- and aminopyridines [17,18], salicylaldiminato ligands [19], various organic acids [20–30], and derivatives of (di)picolinic acid [31].

For copper systems, a linear relationship between the reduction potential of the copper complex and the logarithm of the equilibrium constant or the logarithm of the apparent rate constant ($k_p^{app} = k_p[R^{\bullet}]$) has been shown [32–37]. A lower (more negative) reduction potential of the copper complex (i.e. a more active mediator) results in a higher equilibrium constant and apparent rate

* Corresponding author. Tel.: +46 8 790 9279; fax: +46 8 790 8772.
E-mail address: hebe@kth.se (H. Bergenudd).

1381-1169/$ – see front matter © 2011 Elsevier B.V. All rights reserved.
doi:10.1016/j.molcata.2011.06.001

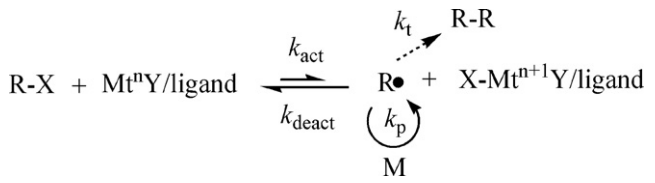

Scheme 1. General mechanism for ATRP.

constant for propagation. Although the reduction potentials of some iron complexes have been measured in acetonitrile and qualitative comparisons have been made between the potentials and the polymerization results [15–19], a quantitative correlation between the potential and the logarithm of the apparent rate constant, as for copper complexes, has not been reported for iron complexes.

Understanding the effect of different ligands on the ATRP system with iron is as important as it is for copper systems, not least in the search for more environmental friendly ligands. In this work we report on the investigation of the redox properties of some iron complexes and their behavior in normal and reverse ATRP of MMA in DMF. To avoid complications in the data interpretation due to heterogeneity, DMF was chosen as the solvent to ensure complete solubility of all the ligands and complexes used in this study in both electrochemical measurements and polymerizations.

2. Experimental

2.1. Materials

Methyl methacrylate (MMA, 99%, Aldrich) was passed through a column of neutral alumina prior to polymerization. *N*,*N*-Dimethylformamide (DMF, ≥99%, VWR Int.), ethyl acetate (EtOAc, z.A., Merck), anhydrous $FeCl_2$ (99.5%, Alfa Aesar), $FeCl_3{\cdot}6H_2O$ (z.A., Merck), $CuBr_2$ (≥99%, Sigma–Aldrich), L-ascorbic acid (≥99%, Fluka), azobisisobutyronitrile (AIBN, ≥98%, Fluka), 2,2′-bipyridine (bipy, 99+%, Aldrich), *N*,*N*,*N*′,*N*″,*N*″-pentamethyldiethylenetriamine (PMDETA, 99%, Aldrich), triphenylphosphine (PPh_3, ≥98.5%, Fluka), isophthalic acid (IPA, ≥98%, Aldrich), iminodiacetic acid (IDA, ≥98%, Fluka), dipicolinic acid (PDA, 99%, Aldrich), oxalic acid (98%, Aldrich), 2-picolinic acid (PA, Nobel Chemicals), tetrabutylammonium tetrafluoroborate (Bu_4NBF_4, ≥98%, Fluka), ferrocene (98%, Alfa Aesar) and ethyl 2-bromoisobutyrate (EBiB, 98%, Sigma Aldrich) were used as received.

2.2. Cyclic voltammetry

Cyclic voltammetry was performed with a PAR 263A potentiostat/galvanostat interfaced to a base PC using the EG&G Model 270 software package. The cell was a standard three-electrode setup using a 2 mm diameter glassy carbon working electrode, a platinum coil counter electrode and a saturated calomel reference electrode. Full IR compensation was employed in all measurements. All measurements were performed in DMF with 0.1 M Bu_4NBF_4 as supporting electrolyte. The half-wave potential ($E_{1/2}$) of ferrocene (1 mM) was 490 mV. The iron complexes were measured at 3 mM concentration, using a saturated calomel electrode (SCE) as reference electrode, and the scan rate was 1000 mV/s. All potentials are reported vs. SCE. In most cases, the iron:ligand ratio was 1:2, except for PMDETA where it was 1:1.

2.3. UV–vis spectroscopic analyses

UV–vis spectroscopy was used to analyze iron complexes in DMF and DMF + EtOAc (ethyl acetate) on a Jasco V-630 spectrophotometer. Samples of $FeCl_3$, $FeCl_3$/IPA, $FeCl_3$/PPh_3, $FeCl_2$/IPA and $FeCl_2$/PPh_3 (all 2 mM, Fe/ligand = 1/2) were prepared in DMF. The absorbance was measured between 270 and 1100 nm. The samples with $FeCl_2$/ligand were prepared under inert atmosphere and measured immediately. They were then exposed to air and the absorbance was measured again after oxidation (denoted "ox"). In addition, one sample was prepared to resemble a polymerization mixture. $FeCl_2$/IPA (25 mM) and the ATRP initiator EBiB (25 mM) were added to a 1:1 mixture of DMF and EtOAc (which was used instead of MMA, being similar in structure) under inert atmosphere in a glass vial. The sample was heated to 50 °C for 3 h. The color change from lightly yellow-brown to orange indicated that the iron complex had reacted with the initiator. The absorbance was measured after the reaction, both for a sample which was not exposed to air and one that was removed from the closed vial and exposed to air (which resulted in a color change to dark orange). For all samples measured, dilution was required due to the high absorbance below 450 nm.

2.4. General procedure for normal ATRP

In all polymerizations, the targeted DP was 200 and the amount of solvent (DMF) was 50% (w/w). $FeCl_2$ (0.25 mmol, 31.7 mg) was charged into a dry round-bottomed flask equipped with a magnetic stirring bar. The flask was sealed with a rubber septum and degassed by purging with argon for 20 min. A separately degassed solution of ligand (0.5 mmol (0.25 mmol for PMDETA)) in DMF (5 g) was added via a degassed syringe and the resulting solution was stirred until all $FeCl_2$ was dissolved. The initiator (EBiB, 0.25 mmol) was mixed with MMA (50 mmol, 5 g), the solution was purged with argon and then added to the round bottomed flask containing the DMF solution with the iron complex. The flask was placed in a thermostated oil bath at the desired temperature. Aliquots were withdrawn with a degassed syringe at timed intervals, diluted in toluene or ethyl acetate and passed through a small column of neutral alumina to remove the iron complex. Conversion was followed by ^{1}H NMR and the molecular weights were analyzed by SEC.

2.5. General procedure for reverse ATRP

The procedure for reverse ATRP was the same as for normal ATRP, except that the initiator, AIBN (0.125 mmol, 20.5 mg), was added to the round-bottomed flask together with $FeCl_3{\cdot}6\ H_2O$ (0.25 mmol, 67.6 mg).

2.6. General procedure for AGET ATRP

The procedure for AGET ATRP with iron chloride was the same as for normal ATRP in general. $FeCl_3{\cdot}6\ H_2O$ (0.25 mmol, 67.6 mg), PPh_3 (0.5 mmol, 131.1 mg) and DMF (3 g) were charged into a round bottomed flask and ascorbic acid (0.125 mmol, 22 mg) was dissolved separately in DMF (2 g) and added to the flask after degassing both solutions. EBiB (0.25 mmol, 48.8 mg) was used as initiator.

2.7. General procedure for chain extension with AGET ATRP from macroinitiator

The macroinitiator was PMMA-X (X = Cl or Br) prepared through normal or reverse ATRP with one of the iron complexes, precipitated into MeOH and dried. The targeted DP in the chain extensions was 500. A stock solution of $CuBr_2$ (6.3 mM) and PMDETA (6.3 mM) in DMF was prepared and degassed with argon, after which ascorbic acid (3.1 mM) was added to reduce the copper complex. The macroinitiator (0.03 mmol), DMF (0.4 g) and MMA (1.4 g) were charged into a round-bottomed flask, which was then sealed with a rubber septum, and stirred until the macroinitiator was completely

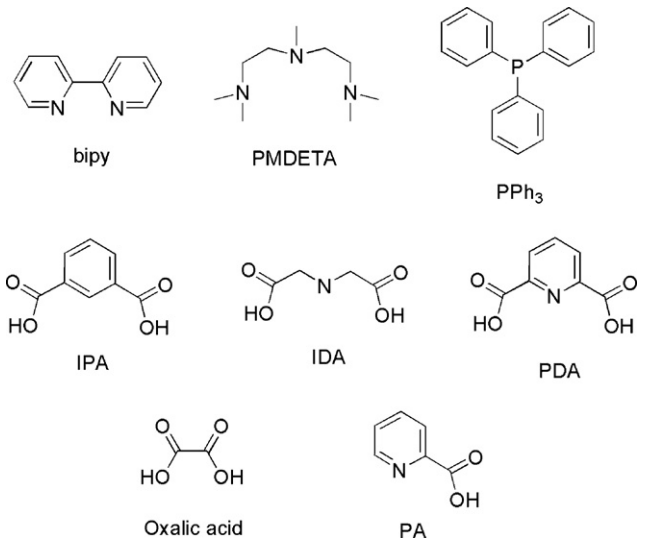

Fig. 1. Structures of the ligands of the iron complexes.

dissolved. After purging with argon for 30 min, 1.4 g of the copper/PMDETA stock solution was added via a degassed syringe. The flask was placed in a thermostated oil bath at 70 °C. After the polymerization was stopped, the resulting polymer was precipitated into MeOH, filtered and dried.

2.8. Characterization

^{1}H NMR spectra were recorded on a Bruker Avance 400 MHz NMR instrument using $CDCl_3$. Size Exclusion Chromatography (SEC) using THF (1.0 mL min^{-1}) as the mobile phase was performed at 35 °C using a Viscotek TDA model 301 equipped with two GMH_{HR}-M columns with TSK-gel (mixed bed, MW resolving range: 300–100,000) from Tosoh Biosep, a VE 5200 GPC autosampler, a VE 1121 GPC solvent pump, and a VE 5710 GPC degasser (all from Viscotek corp.). A conventional calibration method was created using narrow linear polystyrene standards. Corrections for the flow rate fluctuations were made using toluene as an internal standard. Viscotek OmniSEC version 4.0 software was used to process the data. The error in the molecular weight due to the difference in hydrodynamic volume between the polystyrene standards and the measured PMMA was estimated to ≤10%.

3. Results and discussion

To investigate the relationship between the reduction potential and the polymerization behavior for iron complexes, eight ligands with different structures and binding groups were chosen (Fig. 1). The chosen ligands contain a few different functional groups: pyridine units (bipy, PDA and PA), amines (PMDETA and IDA), carboxylic acids (oxalic acid, IPA, IDA, PDA and PA) and phosphines (PPh_3). The intent was to get a good spread in reduction potentials, as previously for copper complexes [32–36]. In mechanistic investigations, it is crucial to have a homogeneous system, since heterogeneity causes uncertainties regarding the concentration of active species, and interfacial processes can complicate the interpretation of experimental data significantly [38]. To ensure complete solubility of all ligands and complexes in both the polymerizations and the investigation of the redox properties, DMF was chosen as the solvent. DMF has been used as solvent in ATRP of MMA with iron complexes in several other reports [20,23,25–31,39].

3.1. Cyclic voltammetry

The redox properties of the eight ligands in combination with $FeCl_2$ were measured with cyclic voltammetry in DMF. $FeCl_2$ alone, as well as $FeCl_3$, were also run for comparison. The redox processes were not reversible, as seen by the large peak-to-peak separation values ($\Delta E = E_{ox} - E_{red}$) being much larger than the ideal 60 mV for a one-electron-transfer process. The currents for $FeCl_2$ were low compared to ferrocene, but increased some when ligands were added, although still lower than for ferrocene. The reason for this could be different electron transfer efficiency for different substances. $FeCl_3$ also displayed larger currents for the oxidation and reduction processes than $FeCl_2$. The reduction and oxidation potentials did not differ significantly between $FeCl_2$ and the iron complexes in most cases, E_{red} being close to 0 mV and E_{ox} approximately 360 mV. Some examples of voltammograms are shown in Fig. 2. Using $FeCl_3$ instead of $FeCl_2$ to form the complexes did not change the general appearance of the voltammograms. For $FeCl_2$/PMDETA, the oxidation potential was slightly more positive than for $FeCl_2$, E_{ox} = 430 mV, but no reduction peak appeared in the voltammogram (Fig. 2A). The voltammograms of $FeCl_2$/PDA exhibited several oxidation and reduction peaks (Fig. 2A). Besides the peaks at 0 and 360 mV, there was also a nearly reversible process at $E_{1/2}$ = −280 mV (ΔE = 70 mV). This process did, however, not seem to affect the polymerization with this iron complex, *vide infra*. The oxidation peaks of $FeCl_2$/IPA and $FeCl_2$/PA both displayed a shoulder at a slightly lower potential (Fig. 2B), which could indicate the presence of more than one structure of the iron complex, e.g. different numbers of ligands bound to the central iron. In fact, with a 1:2 ratio of $FeCl_2$:PA, the oxidation peak indicated by the shoulder is dominating. With $FeCl_2$/bipy, the oxidation and reduction peaks in the measurement with a 1:1 ratio were similar to $FeCl_2$. However, adding a second equivalent of the ligand (Fe/L = 1:2) resulted in a disappearance of these peaks and the appearance of reversible redox process at $E_{1/2}$ = 1100 mV (Fig. 2C), which corresponds to the $Fe(bipy)_3^{2+}$ complex [40]. The color of the Fe/bipy solution (both 1:1 and 1:2) is red, which is consistent with the $Fe(bipy)_3^{2+}$ complex. The reduction peak for $FeCl_2$/IDA was relatively broad and shifted towards more negative potentials compared to $FeCl_2$ (Fig. 2D).

Since the potentials are the same with and without ligand in most cases, it seems that the ligands do not bind to iron. This is a bit surprising, since the iron complexes with PPh_3 [41,42] and PMDETA [43] have been isolated and characterized. However, electrochemical studies of other iron complexes in DMF have indicated that only Fe(III) forms complexes, as only the reduction peak was affected by ligand addition [44,45]. It is well known that iron is complexed by DMF [46,47] and if the binding constant for an added ligand is not large enough, ligand exchange with DMF will not take place.

3.2. Polymerizations

Six of the ligands were tested in polymerizations of MMA (IDA was not used due to insolubility in the polymerization medium). Normal ATRP was performed at 65 °C and 90 °C, whereas reverse ATRP was only run at 90 °C in order to obtain a fast dissociation of the thermal initiator (i.e. AIBN). AGET ATRP, with ascorbic acid as reductant, was also run at 90 °C.

The initial apparent rate constants with the various ligands do not differ more than a factor two within the same ATRP system (Table 1). This is consistent with the electrochemical measurements, where the redox potentials were practically unaffected by the choice of ligand. The bipy system was heterogeneous, which caused a lower apparent rate constant compared to the other ligands. With the high redox potential found for the Fe/bipy complex at a 1:2 ratio (*vide supra*) it could be expected that the polymerization would be very slow (a more than two orders of magnitude

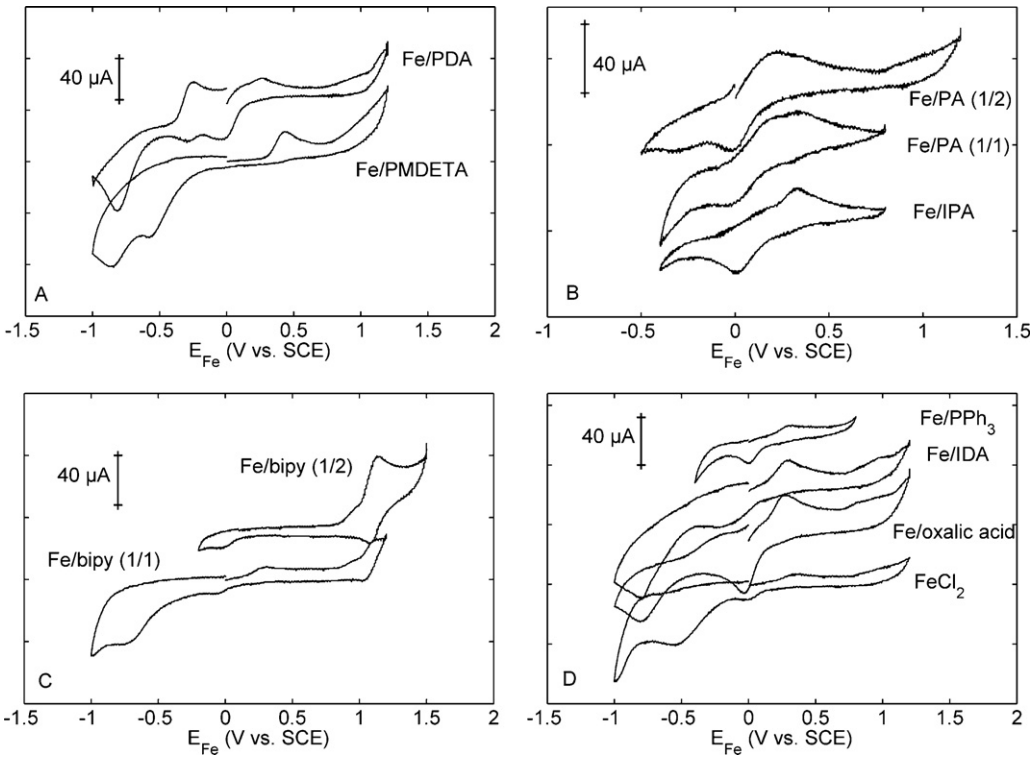

Fig. 2. Cyclic voltammograms of $FeCl_2$/ligand complexes in DMF (0.1 M Bu_4NBF_4, scan rate: 1000 mV/s and $[Fe]_0$ = 3 mM).

lower apparent rate constant), which is not the case, however, indicating that the $Fe(bipy)_3^{2+}$ complex is not responsible for the activation process. The reversible redox process at lower potentials for Fe/PDA could be expected to increase the apparent rate constant for that system, but as the apparent rate constant with Fe/PDA did not deviate from the other iron complexes, this process appears to be insignificant in the polymerization.

For the reverse ATRP systems, the apparent rate constants are lower than in normal ATRP at the same temperature. However, the degree of control is significantly improved for reverse ATRP compared to normal ATRP. The kinetics is first order for all the reverse ATRP systems, whereas curvature is found in all the normal ATRP systems. The kinetics for the ATRP systems with PPh_3 are shown in Fig. 3. The apparent rate constants and the degree of control in AGET ATRP are similar to reverse ATRP.

This difference in the degree of control is also seen with the molecular weights (Table 2). For the reverse ATRP systems and AGET ATRP, the molecular weights increase linearly with conversion and are close to the theoretical molecular weight ($M_{n,th} = conv \cdot DP \cdot M_{mon}$) (Figs. S1 and S2). For the other polymerizations, however, the molecular weights are high and constant throughout the polymerization. Examples are found in Figs. 4 and 5. The number average molecular weights appear to decrease with conversion for the polymers prepared by normal ATRP, see Fig. 4. However, as can be seen from the GPC traces for the same polymer in Fig. 5, this is an effect of an increasing fraction of lower molecular weight chains. The molecular weights are practically constant with time. It is possible that the bimodal shape of the GPC traces for the polymer from normal ATRP is the consequence of early terminations, resulting in the shift of the bimodal curve towards higher

Table 1
Initial apparent rate constants for normal, AGET and reverse ATRP of MMA with iron complexes.[a]

Ligand	Added $FeCl_3$ [b]	k_p^{app} ($\times 10^{-5}$ s^{-1})[c]		
		65 °C	90 °C	Reverse
–		9.2		6.0
bipy		2.8		
IPA		6.6	23.1	5.2
PA		4.2	11.8	4.9
PDA		4.7		
PMDETA		3.9		
PPh_3		8.6	29.3	8.8
PPh_3	5%	8.1		
PPh_3	50%	0.4		
PDA	50%	0.3		
PPh_3			6.1[d]	

[a] Initiators = EBiB (normal and AGET ATRP, $[MMA]_0:[I]_0:[Fe]_0$ = 200:1:1), AIBN (reverse ATRP, $[MMA]_0:[I]_0:[Fe]_0$ = 200:0.5:1), 50% (w/w) DMF.
[b] In percent of $[FeCl_2]_0$.
[c] k_p^{app} for normal ATRP at 65 °C and 90 °C and for reverse and AGET ATRP (at 90 °C).
[d] AGET ATRP, $[Fe]_0:[AscAc]_0$ = 1:0.5.

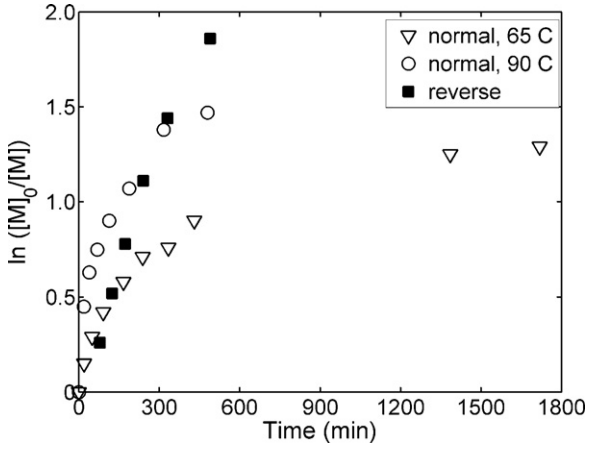

Fig. 3. Kinetic plots for the normal (at 65 or 90 °C, with EBiB initiator) and reverse (at 90 °C, with AIBN as initiator) ATRP of MMA with $FeCl_x/PPh_3$ (x = 2 or 3). For other experimental conditions, see Table 1.

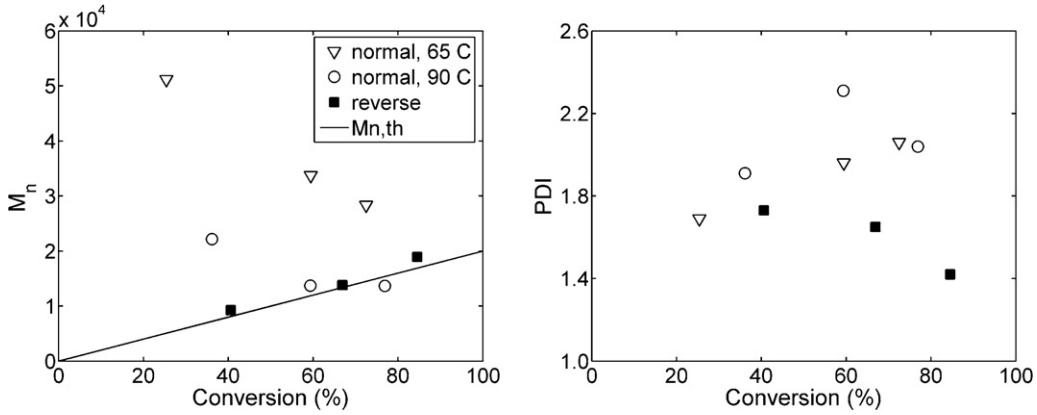

Fig. 4. Molecular weights and PDI-values for PMMA prepared by normal and reverse ATRP with $FeCl_2/PPh_3$ (normal ATRP) or $FeCl_3/PPh_3$ (reverse ATRP). For experimental conditions, see Table 1.

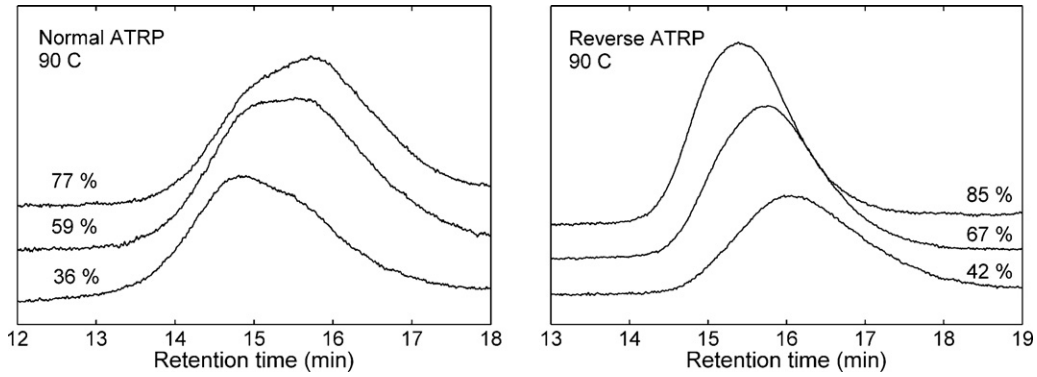

Fig. 5. GPC traces from normal and reverse ATRP of MMA with $FeCl_2/PPh_3$ (normal ATRP) or $FeCl_3/PPh_3$ (reverse ATRP), at different conversions. The M_n and PDI data can also be seen in Fig. 4. For experimental conditions, see Table 1.

molecular weights at lower conversions. The GPC traces for the polymers from normal ATRP all had a similar shape as in Fig. 5.

One reason for good control in the reverse ATRP systems can be that the initiation is not complete. That is, if a significant portion of the initiator molecules terminate initially, some of the Fe(III) is not converted to Fe(II), and hence, the ATRP equilibrium is shifted towards the dormant species. In AGET ATRP, non-quantitative reduction of Fe(III) by ascorbic acid would also result in a shift towards the dormant species (although an increased amount of ascorbic acid, so that Fe(III):ascorbic acid = 1:1, did not

Table 2
Molecular weights and PDI-values for normal, AGET and reverse ATRP with iron complexes.[a]

Ligand	Initiator	$FeCl_3$ [b]	*Conv* (%)	$M_{n,th}$	M_n	PDI
Reverse ATRP						
IPA	AIBN		88	17,600	17,700	1.4
PA	AIBN		75	14,900	15,200	1.4
PPh_3	AIBN		85	16,900	18,900	1.4
–	AIBN		73	14,600	16,700	1.4
Normal ATRP, 65 °C						
–	EBiB		58	11,500	28,400	2.0
bipy	EBiB		64	12,800	62,600	2.6
IPA	EBiB		48	9500	25,200	1.8
PA	EBiB		50	10,000	19,800	1.5
PDA	EBiB		29	5800	23,700	1.5
PDA	EBiB	50%	23	4600	12,500	1.3
PMDETA	EBiB		28	5600	115,000	2.5
PPh_3	EBiB		59	11,900	33,700	2.0
PPh_3	EBiB	5%	68	13,700	25,300	1.7
PPh_3	EBiB	50%	53	10,500	6300	1.7
Normal ATRP, 90 °C						
IPA	EBiB		65	12,900	13,800	2.2
PA	EBiB		62	12,400	9700	1.7
PPh_3	EBiB		77	15,400	13,700	2.0
AGET ATRP, 90 °C						
PPh_3	EBiB		76	15,200	15,800	1.3

[a] For experimental conditions, see Table 1.
[b] In percent of $[FeCl_2]_0$.

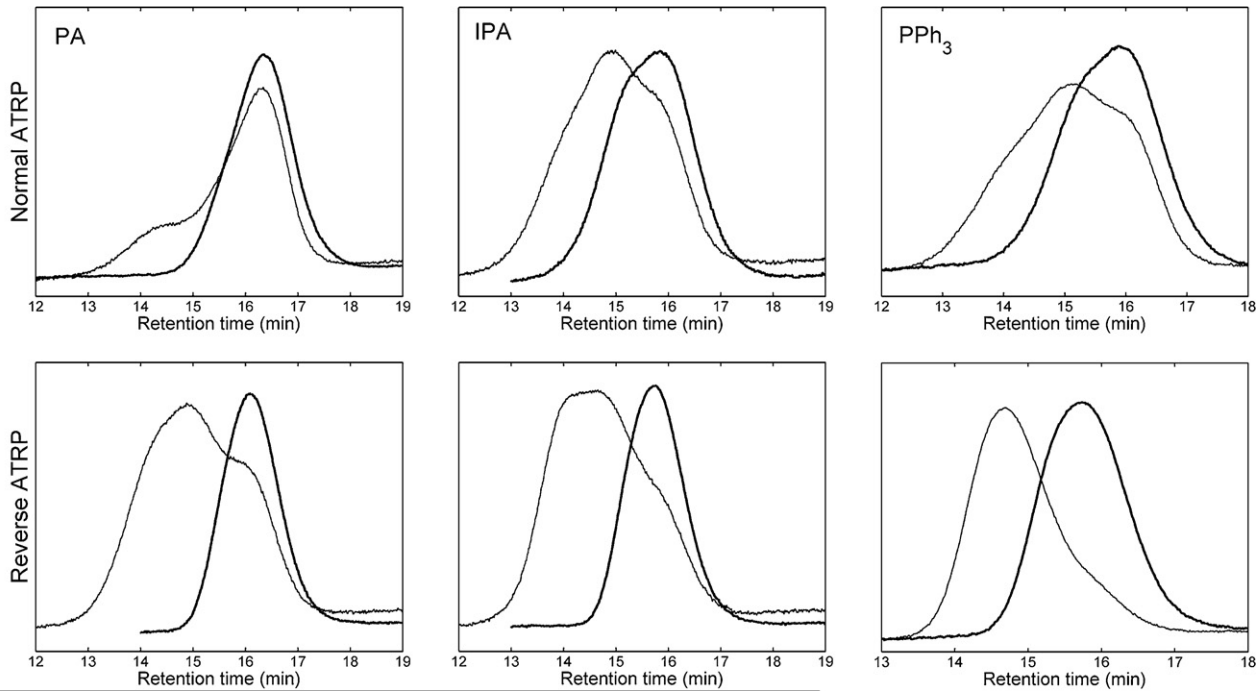

Fig. 6. GPC traces of macroinitiators (thick lines), prepared by normal (90 °C) or reverse ATRP with iron complexes (ligands as indicated), and chain extended polymers (thin lines).

alter the degree of control). The initiator efficiency for AIBN is in the order of 0.6 [48]. Hence, if only 60% of the initiators give rise to a polymer chain, the amount of Fe(III) would be significant and the molecular weights would be expected to be significantly above the theoretical molecular weights. However, the molecular weights are very close to the theoretical molecular weights, indicating that practically all initiator molecules have started a polymer chain. Also, with 50% $FeCl_3$ (relative to $[FeCl_2]_0$) added in normal ATRP, the apparent rate constants are reduced (Table 1), but the molecular weights are still constant with conversion, indicating that extra Fe(III) in the normal ATRP system does not increase the degree of control despite the lower radical concentration (lower k_p^{app}).

One explanation for molecular weights close to theoretical in reverse ATRP, if the initiation efficiency for AIBN would only be 60%, could be that Fe(III) species oxidize the monomer. This possibility has been reported for copper and iron mediated ATRP, in systems starting from the transition metal in its higher oxidation state but without the addition of a reductant [49–52]. The suggested mechanism for the reduction of MMA in copper systems results in a halogenated monomer, similar in structure to ATRP initiators [49]. This halogenated monomer species could possibly act as initiator, thus increasing the total initiation efficiency in the present system, but initiation with this species has not been confirmed in the literature so far. Also, if this occurs in the present system for reverse ATRP, the total initiation efficiency would still only be 80% (assuming 60% initiation efficiency of AIBN), which would result in a visible deviation from the theoretical molecular weight (in the suggested mechanism, two Cu(II) species oxidize on MMA molecule [49]). There are also two important differences between the present systems and those reported by other groups. In three of the reports, common ATRP initiators (i.e. alkyl halides like EBiB) are present, which enables activation by the reduced mediator. This is not possible in the reverse ATRP systems. In addition, the majority of the reported polymerizations where oxidation of MMA is suggested are performed in non-polar solvents such as toluene. In DMF however, it can be expected that the reduction potentials are different compared to toluene due to the difference in polarity. Therefore, the oxidation of MMA by Fe(III) species to generate initiating species may not be possible at all in DMF.

Constant molecular weights throughout the polymerization, which was seen in the normal ATRP systems, can be caused by e.g. catalytic chain transfer (CCT) or some other reaction between the growing polymer chain and the iron complex (*vide infra*). The PDI-values are not very low in any of the polymerizations, but the reverse ATRP systems have relatively narrow molecular weight distributions, which decrease during the polymerization.

The results from attempts to perform chain extension from polymers prepared by normal and reverse ATRP were inconclusive. Since the macroinitiators were isolated at the end of the polymerizations, it is probable that a large fraction of the chains from normal ATRP were terminated as assessed from the strong curvature in the kinetic plots. The macroinitiators prepared by reverse ATRP increased significantly in molecular weight, but with broad or bimodal distributions. The macroinitiators from normal ATRP did not grow to any larger extent. GPC traces of the results from the chain extensions are shown in Fig. 6.

^{1}H NMR spectroscopy was used to characterize the end groups of the dry polymers, see Fig. 7, for typical spectra of PMMA prepared by normal and reverse ATRP (with IPA as the ligand). The signal at 3.76 ppm (peak c) is attributed to the methyl ester group at the halogen containing chain end. This signal was stronger for PMMA prepared by reverse ATRP, indicating fewer active chain ends in PMMA from normal ATRP. The signal at 2.5 ppm (peak d) is attributed to the $-CH_2-$ group adjacent to the halogen containing chain end and is present in PMMA from both normal and reverse ATRP. As can also be seen in Fig. 7, the methyl group in the initiator EBiB is present at 4.1 ppm (peak a) in the PMMA prepared by normal ATRP. These peak assignments are similar to those reported by Zhang et al. and Ando et al. [29,53]. A small peak at 1.26 ppm for PMMA from reverse ATRP was assigned to the residue from the AIBN initiator. Weak signals at 5.56 and 6.10 ppm were also present in PMMA samples from both normal and reverse ATRP. These peaks could be attributed to the vinyl protons of the unsat-

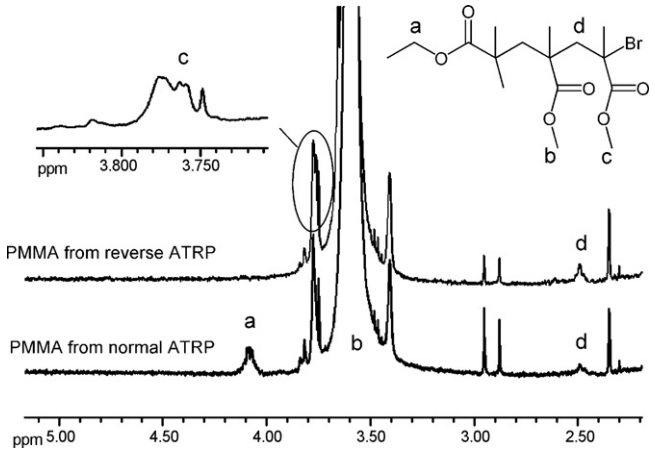

Fig. 7. ^{1}H NMR spectrum of PMMA prepared by normal and reverse ATRP at 90 °C with iron/IPA ($M_n \sim 20{,}000$ g/mol).

urated chain end, but it is also possible that they originate from residual monomer.

3.3. UV–vis spectroscopy

UV–vis spectroscopy was used to analyze some of the iron complexes. The ligands investigated were PPh_3 and IPA together with either $FeCl_3$ or $FeCl_2$. In most cases, DMF was used as solvent. One solution was also prepared to resemble a polymerization solution in order to study the Fe(III) species resulting from Fe(II) species being oxidized through the activation of EBiB. The solvent was then DMF/EtOAc (50/50 by weight), where EtOAc was used instead of MMA to avoid polymerization but still having similar properties of the solution as in the polymerizations. The solutions were initially prepared at a 2 mM concentration (25 mM with EBiB), but the absorbance was too high at wavelengths below 450 nm wherefore all solutions were diluted to 0.2 mM or lower. The UV–vis spectra of the iron complexes with IPA are shown in Fig. 8. The results for Fe/PPh_3 were similar to those with Fe/IPA.

Firstly, the spectrum of $FeCl_3$/IPA is very similar to that of $FeCl_3$, besides the peaks below 300 nm which belong to the ligand (IPA). This indicates that the Fe(III) species do not bind to the added ligand (IPA) to any appreciable extent. The results for $FeCl_3/PPh_3$ were similar, but with less distinct peaks between 300 and 450 nm. The peaks in the spectrum for oxidized iron species resulting from exposing the $FeCl_2$/IPA mixture to air ($FeCl_2$/IPA ox) were less well-defined than in the $FeCl_3$ spectra (Fig. 8B). Although the absorbance is much lower for $FeCl_2$/IPA ox, it appears to be similar to $FeCl_3$/IPA at 360 nm, whereas there appears to be a small shift towards shorter wavelengths compared to $FeCl_3$/IPA near 316 nm. The results for the solution where $FeCl_2$/IPA reacted with EBiB were similar to those with $FeCl_2$/IPA, but it was difficult to see whether the peak indicated by a shoulder near 316 nm is similar to $FeCl_3$/IPA or not (Fig. 8B). At wavelengths below 300 nm, the $FeCl_2$/IPA + EBiB solution displayed high absorption, but without the distinct pattern of the ligand (Fig. 8A and B). There is also a difference in peak height between $FeCl_2$/IPA + EBiB and $FeCl_3$/IPA in Fig. 8B, which could indicate different Fe(III) speciation. (The spectrum of $FeCl_2$/IPA + EBiB was the same whether measured before or after exposing the reaction mixture to air. Also, the spectra of the samples exposed to air, i.e. $FeCl_2$/IPA with or without EBiB, did not change after letting the samples stand for several days exposed to the surroundings.) It should be noted that the spectrum of $FeCl_3$/IPA did not differ between a DMF solution and a DMF/EtOAc solution. Upon dilution, new peaks at wavelengths around 500 nm appeared (Fig. 8C) which have not been assigned to any structure, however. The concentration of ligand relative to solvent is lower during the UV–vis measurements compared to the polymerizations, both before and after dilution. It is thus possible that the new peaks around 500 nm and the similarity between $FeCl_3$ with and without ligand is the result of a relative decrease in ligand concentration. However, increasing the ligand concentration significantly did not change the appearance of the peaks. For the solution with $FeCl_2$/IPA + EBiB, dilution to less than 0.2 mM was required to see a peak in the 500 nm region. It is obvious, however, that the peaks appearing between 450 and 600 nm were different depending on whether the starting material was Fe(II) or Fe(III), with a shift towards shorter wavelengths in solutions with oxidized Fe(II) species.

Although the peaks originating from oxidized Fe(II) species were less distinct than those from Fe(III) species, which makes it difficult to compare them, there appears to be a slight difference between the Fe(III) species in the two cases. UV–vis spectra of $FeCl_2$/IPA during a polymerization of MMA in DMF have been recorded by Zhu and Yan [20]. These were not compared to $FeCl_3$, but the peaks appear similar to those of $FeCl_3$ in this work.

4. Discussion

This study intended to increase the understanding of how different ligands affect the properties of an ATRP system with iron as the mediator. Although the normal ATRP systems did not behave ideally, the difference between the normal and reverse ATRP systems warrants a discussion of the role of the iron complexes in these systems.

As mentioned earlier, DMF was chosen as the solvent to ensure complete solubility of all ligands and complexes, since a homogeneous system is necessary in a mechanistic investigation such as this. It is well known that DMF coordinates to iron chloride, but also that e.g. bipy, 1,10-phenanthroline (phen) and PPh_3 form complexes with iron and can replace DMF molecules in the coordination

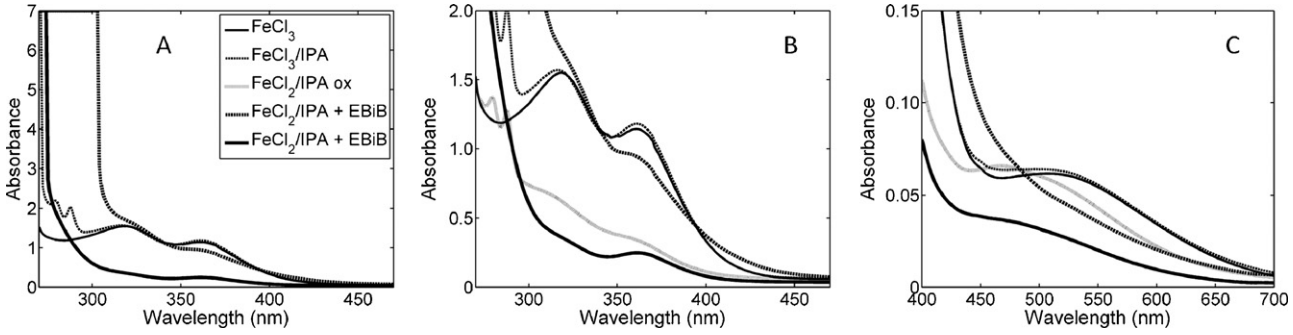

Fig. 8. UV–vis spectra of iron complexes with IPA in DMF or DMF/EtOAc ($FeCl_2$/IPA + EBiB). Concentrations = 0.2 mM, thick solid line ($FeCl_2$/IPA + EBiB) = 0.06 mM. Fe/ligand ratios = 1/2.

sphere. Both bipy and phen are bidentate and the replacement of DMF is entropically favorable. It was therefore expected that the ligands in this study would form complexes with iron chloride in DMF. However, the results from cyclic voltammetry showed that the influence from the ligands on the potentials were insignificant (except in some cases where additional peaks appeared in the voltammograms, although that did not appear to affect the polymerization results). This is very different from copper complexes, where the redox properties in DMF vary significantly with the ligands [34,36]. Since DMF is able to compete with the ligands for the coordination sites on iron, which is also augmented by the higher concentration of DMF compared to the ligands, the influence from the coordinated DMF molecules on the properties of the iron complex dominates over the influence form the other ligands in this study (if they are coordinated at all). The results from the UV–vis study further support that the ligands do not affect the iron complex properties significantly, as the spectra of $FeCl_3$ were similar with and without ligand added. However, some interaction between the ligands and Fe(III)-species was seen in the polymerizations, where the polymerization mixtures during normal ATRP became heterogeneous during the polymerization when no ligand was added, presumably due to limited solubility of Fe(III)-species formed, whereas the mixtures stayed homogeneous when ligands were present. Recently, ATRP of MMA in DMF with $FeBr_2$ as the mediator, without ligands added, was reported [39].

There is also evidence of different Fe(III)-species in normal and reverse/AGET ATRP. Both reverse and AGET ATRP were much better controlled than normal ATRP. The possibility of incomplete initiation in reverse ATRP (or incomplete reduction in AGET ATRP) as an explanation for the good control was discussed above, but the contribution from differences in iron speciation cannot be ruled out. During the polymerizations, there was a color difference between normal and reverse ATRP. Whereas the polymerization mixtures became orange during normal ATRP, presumably from the formation of Fe(III)-species, the starting color in the polymerization mixtures for reverse ATRP were yellow. A small difference between $FeCl_3$/IPA and $FeCl_2$/IPA + EBiB (i.e. Fe(III) species resulting from the activation of EBiB) was also seen in the UV–vis spectra. Another observation was that normal ATRP without ligands became heterogeneous after some time (as mentioned above), but no such difference in homogeneity with and without ligands was seen in the reverse ATRP systems. These differences in color, UV–vis spectra and homogeneity show that the Fe(III) species in normal and reverse ATRP are not the same. That is, the Fe(III)-species resulting from oxidation of Fe(II) in normal ATRP are not the same as the starting Fe(III) species in reverse ATRP. Although the equilibria for ligand exchange (DMF vs. ligand) should be the same for Fe(II) and Fe(III), respectively, irrespective of starting point, it is possible that the coordination sphere around the iron atom is different in the two systems, resulting in exchange equilibria that are shifted in one or the other direction depending on starting material and what is already coordinated to iron.

As mentioned earlier, the constant molecular weights with conversion seen in normal ATRP as opposed to linearly increasing molecular weights in reverse and AGET ATRP can be the result of chain transfer mechanisms. Fe(III)-species are known to terminate polystyrene radicals by hydrogen transfer, leaving unsaturated polymer chain ends [54,55] and chain transfer by iron complexes has been reported for ATRP of styrene and MMA [16,56]. Gibson et al. reported that the spin state of the iron mediator had significant effect on the polymerization outcome [56–58]. High spin complexes afforded ATRP of MMA, whereas intermediate spin complexes resulted in CCT with molecular weights that were constant with conversion. There are similarities between the results presented by Gibson et al. and the present results for normal ATRP of MMA, but a difference is that the molecular weights obtained in this work are much higher (in the order of 20,000 g/mol) than those obtained in the cited work (around 4000 g/mol). Thus, the differences in Fe(III) speciation can have its origin in the spin state of the iron species, resulting in the observed differences between normal and reverse ATRP.

In conclusion, the results from this study show that with DMF as the solvent in ATRP systems with iron, differences in iron speciation govern the outcome of the polymerizations in normal and reverse ATRP. However, the nature of the ligands is not crucial for the properties of the system, i.e. redox properties and polymerization performance. Reasonably well controlled ATRP systems were shown for reverse ATRP, where it is also possible to run the polymerization without ligands.

5. Conclusions

The redox properties of the investigated iron complexes, measured by cyclic voltammetry, were practically the same, which was reflected in the ATRP kinetics. The apparent rate constants did not differ more than a factor two within the same ATRP system (i.e. normal and reverse ATRP). This demonstrates that the nature of the ligand is not very important in this ATRP system. However, the degree of control was much higher in reverse ATRP compared to normal ATRP. Observations during the polymerizations, e.g. homo-/heterogeneity, color and molecular weights, as well as differences in the UV–vis spectra, show that the Fe(III) speciation is different in the two systems, i.e. that the starting Fe(III) species in reverse ATRP differ from the Fe(III) species resulting from oxidation of Fe(II) in normal ATRP. This can, at least in part, be attributed to the chosen solvent, i.e. DMF, known to coordinate to iron and which can thus compete with the ligands for the coordination sites.

Acknowledgement

The Swedish Research Council is acknowledged for financial support.

Appendix A. Supplementary data

Supplementary data associated with this article can be found, in the online version, at doi:10.1016/j.molcata.2011.06.001.

References

[1] W.A. Braunecker, K. Matyjaszewski, Prog. Polym. Sci. 32 (2007) 93–146.
[2] A. Goto, T. Fukuda, Prog. Polym. Sci. 29 (2004) 329–385.
[3] D.A. Shipp, Polym. Rev. 45 (2005) 171–194.
[4] J.-S. Wang, K. Matyjaszewski, Macromolecules 28 (1995) 7572–7573.
[5] W. Jakubowski, K. Matyjaszewski, Macromolecules 38 (2005) 4139–4146.
[6] W. Jakubowski, K. Min, K. Matyjaszewski, Macromolecules 39 (2006) 39–45.
[7] A.J. Carmichael, D.M. Haddleton, S.A.F. Bon, K.R. Seddon, Chem. Commun. (2000) 1237–1238.
[8] M. Ouchi, T. Terashima, M. Sawamoto, Chem. Rev. 109 (2009) 4963–5050.
[9] T. Ando, M. Kamigaito, M. Sawamoto, Macromolecules 30 (1997) 4507–4510.
[10] C. Uchiike, T. Terashima, M. Ouchi, T. Ando, M. Kamigaito, M. Sawamoto, Macromolecules 40 (2007) 8658–8662.
[11] K. Ibrahim, B. Löfgren, J. Seppälä, Eur. Polym. J. 39 (2003) 939–944.
[12] L. Zhang, Z. Cheng, F. Tang, Q. Li, X. Zhu, Macromol. Chem. Phys. 209 (2008) 1705–1713.
[13] K. Matyjaszewski, M. Wei, J. Xia, N.E. McDermott, Macromolecules 30 (1997) 8161–8164.
[14] G. Moineau, P. Dubois, R. Jerome, T. Senninger, P. Teyssie, Macromolecules 31 (1998) 545–547.
[15] R.K. O'Reilly, M.P. Shaver, V.C. Gibson, A.J.P. White, Macromolecules 40 (2007) 7441–7452.
[16] V.C. Gibson, R.K. O'Reilly, W. Reed, D.F. Wass, A.J.P. White, D.J. Williams, Chem. Commun. (2002) 1850–1851.
[17] R.K. O'Reilly, V.C. Gibson, A.J.P. White, D.J. Williams, Polyhedron 23 (2004) 2921–2928.
[18] V.C. Gibson, R.K. O'Reilly, D.F. Wass, A.J.P. White, D.J. Williams, J. Chem. Soc., Dalton Trans. (2003) 2824–2830.

[19] R.K. O'Reilly, V.C. Gibson, A.J.P. White, D.J. Williams, J. Am. Chem. Soc. 125 (2003) 8450–8451.
[20] S. Zhu, D. Yan, Macromolecules 33 (2000) 8233–8238.
[21] S. Zhu, D. Yan, J. Polym. Sci. A: Polym. Chem. 38 (2000) 4308–4314.
[22] S. Zhu, D. Yan, G. Zhang, M. Li, Macromol. Chem. Phys. 201 (2000) 2666–2669.
[23] S. Zhu, D. Yan, G. Zhang, J. Polym. Sci. A: Polym. Chem. 39 (2001) 765–774.
[24] S. Zhu, D. Yan, G. Zhang, Polym. Bull. 45 (2001) 457–464.
[25] C. Hou, R. Qu, L. Ying, C. Wang, J. Appl. Polym. Sci. 99 (2006) 32–36.
[26] C. Hou, L. Ying, C. Wang, J. Appl. Polym. Sci. 99 (2006) 1050–1054.
[27] C. Hou, R. Qu, C. Ji, C. Wang, C. Wang, J. Polym. Sci. A: Polym. Chem. 44 (2006) 219–225.
[28] C. Hou, J. Liu, C. Wang, Polym. Int. 55 (2006) 171–175.
[29] L. Zhang, Z. Cheng, S. Shi, Q. Li, X. Zhu, Polymer 49 (2008) 3054–3059.
[30] H. Chen, L. Yang, Y. Liang, Z. Hao, Z. Lu, J. Polym. Sci. A: Polym. Chem. 47 (2009) 3202–3207.
[31] G. Wang, X. Zhu, Z. Cheng, J. Zhu, J. Polym. Sci. A: Polym. Chem. 44 (2006) 2912–2921.
[32] J. Qiu, K. Matyjaszewski, L. Thouin, C. Amatore, Macromol. Chem. Phys. 201 (2000) 1625–1631.
[33] K. Matyjaszewski, B. Gobelt, H.-j. Paik, C.P. Horwitz, Macromolecules 34 (2001) 430–440.
[34] G. Coullerez, A. Carlmark, E. Malmstrom, M. Jonsson, J. Phys. Chem. A 108 (2004) 7129–7131.
[35] W. Tang, Y. Kwak, W. Braunecker, N.V. Tsarevsky, M.L. Coote, K. Matyjaszewski, J. Am. Chem. Soc. 130 (2008) 10702–10713.
[36] H. Bergenudd, G. Coullerez, M. Jonsson, E. Malmström, Macromolecules 42 (2009) 3302–3308.
[37] W. Tang, K. Matyjaszewski, Macromolecules 39 (2006) 4953–4959.
[38] H. Bergenudd, M. Jonsson, D. Nyström, E. Malmström, J. Mol. Catal. A: Chem. 306 (2009) 69–76.
[39] Y. Wang, K. Matyjaszewski, Macromolecules 43 (2010) 4003–4005.
[40] M. Ocafrain, M. Devaud, M. Troupel, J. Perichon, Electrochim. Acta 42 (1997) 99–105.
[41] J.D. Walker, R. Poli, Inorg. Chem. 28 (1989) 1793–1801.
[42] O. Seewald, U. Flörke, G. Henkel, Acta Crystallogr. E 61 (2005) m1829–m1830.
[43] F. Calderazzo, U. Englert, G. Pampaloni, E. Vanni, C.R. Acad. Sci. II C 2 (1999) 311–319.
[44] M.T. Escot, P. Pouillen, P. Martinet, C.R. Acad. Sci. II 292 (1981) 665–668.
[45] M.-T. Escot, A.-M. Martre, P. Pouillen, P. Martinet, Bull. Soc. Chim. Fr. 3 (1989) 316–320.
[46] Y.J. Kim, C.R. Park, Inorg. Chem. 41 (2002) 6211–6216.
[47] V.T. Yilmaz, Y. Topcu, Thermochim. Acta 307 (1997) 143–147.
[48] L.M. Arnett, J.H. Peterson, J. Am. Chem. Soc. 74 (1952) 2031–2033.
[49] A.K. Nanda, S.C. Hong, K. Matyjaszewski, Macromol. Chem. Phys. 207 (2003) 1151–1159.
[50] C.R. Becer, R. Hoogenboom, D. Fournier, U.S. Schubert, Macromol. Rapid Commun. 28 (2007) 1161–1166.
[51] Z. Xue, H.S. Oh, S.K. Noh, W.S. Lyoo, Macromol. Rapid Commun. 29 (2008) 1887–1894.
[52] Z. Xue, N.T.B. Linh, S.K. Noh, W.S. Lyoo, Angew. Chem. Int. Ed. 47 (2008) 6426–6429.
[53] T. Ando, M. Kamigaito, M. Sawamoto, Macromolecules 31 (1998) 6708–6711.
[54] N.N. Dass, M.H. George, J. Polym. Sci. A: Polym. Chem. 7 (1969) 269–281.
[55] P.D. Chetia, N.N. Dass, Eur. Polym. J. 12 (1976) 165–168.
[56] V.C. Gibson, R.K. O'Reilly, D.F. Wass, A.J.P. White, D.J. Williams, Macromolecules 36 (2003) 2591–2593.
[57] M.P. Shaver, L.E.N. Allan, H.S. Rzepa, V.C. Gibson, Angew. Chem. Int. Ed. 45 (2006) 1241–1244.
[58] L.E.N. Allan, M.P. Shaver, A.J.P. White, V.C. Gibson, Inorg. Chem. 46 (2007) 8963–8970.